Polish Journal of Medical Physics and Engineering
The Journal of Polish Society of Medical Physics
ISSN 1898-0309, doi: 10.2478/pjmpe-2024-0020

September 2024
Vol 30, Issue 3

Scientific Paper

Quantitative dosimetric analysis with independent software solutions and comprehensive treatment plan parameter evaluation in skin brachytherapy

Michał PÓŁTORAK [1,ABCD,*], Paweł BANATKIEWICZ[1,E], Łukasz PÓŁTORAK[2,EF], Piotr SOBOLEWSKI[3,4,E], Damian ZIMOŃ[3,4,E], Maciej SZWAST[5,CDEF], Irena WALECKA[3,4,F]

[1]*Radiotherapy Center - The National Institute of Medicine of the Ministry of the Interior and Administration, Woloska 137, 02-507, Warsaw, Poland*
[2]*Electrochemistry@Soft Interfaces Team, Department of Inorganic and Analytical Chemistry, Faculty of Chemistry, University of Lodz, Tamka 12, 91-403, Lodz, Poland*
[3]*Dermatology Clinic - The National Institute of Medicine of the Ministry of the Interior and Administration, Woloska 137, 02-507, Warsaw, Poland*
[4]*Department of Dermatology, Centre of Postgraduate Medical Education, 02-507 Warsaw, Poland*
[5]*Department of Chemical and Process Engineering, Warsaw University of Technology, Warynskiego 1, 00-645, Warsaw, Poland*
[*]*Corresponding author: Michał Półtorak; michal.poltorak@cskmswia.gov.pl*

(received 24 May 2024; revised 6 June and 7 July 2024; accepted 11 July 2024)

Abstract

Background and Purpose: This study aimed to investigate quantitative dosimetric analysis with independent software solutions and comprehensive treatment plan parameter evaluation for the treatment of skin cancer. Specifically, we aimed to conduct a dosimetric analysis of the treatment plan and we presented the clinical parameters used in our institution of clinically used treatment plans.

Materials and Methods: This study compares dose calculations between BrachyVision v16.1 and RadCalc v7.2 for brachytherapy applications. It evaluates key treatment plan parameters, including V_{100}, V_{150}, V_{200}, D_{90}, CI, DNR, mean treatment depth, treatment time, and various Gamma values. Dose calculations utilized the 192-Ir GammaMed HDR Plus source. RadCalc employed a referenced model. Applicators were 3D printed using PLA as the printing filament.

Results: The study assessed compliance for 20 patient plans, finding a mean dose difference of 0.05% with a standard deviation of 0.26%. V_{100}, V_{150}, and V_{200} showed high compliance, with V_{100} having a minimal mean difference of 0.01%, a standard deviation of 0.02% and V_{200} exhibiting the lowest compliance 0.52%, a standard deviation of 1.72%. D_{90} values displayed high compliance with a mean difference of 0.35%, and a standard deviation of 1.85%. The coverage index parameter was strongly supported (R^2: 0.984). DNR values indicated close agreement with a mean difference of 0.01%, a standard deviation: of 0.10%. The average Gamma value was 99.91% with a standard deviation of 0.11%.

Conclusion: The agreement between treatment planning system and independent software solutions results validates treatment planning accuracy. This supports the method's suitability for patient care and encourages wider adoption, ensuring quality assurance in clinical settings.

Keywords: 3D printing; skin cancer; individual applicator; independent check; quality assurance; plan parameters.

Introduction

Cutaneous malignancies, notably skin cancer, exhibit a global prevalence marked by a consistent rise in reported cases, prominently involving basal cell carcinoma (BCC) and squamous cell carcinoma (SCC).[1-4] For patients where surgical excision might yield unfavorable outcomes, such as cosmetic or reconstructive issues, brachytherapy stands out as a widely adopted modality for treating skin cancer.[5] This localized radiation therapy has gleaned attention, and the incorporation of 3D printing technology holds significant potential for augmenting precision and efficacy in therapy.[6-11] Surface brachytherapy efficiently targets superficial tumors, achieving a high dose to the tumor volume while minimizing radiation exposure to underlying tissues due to its rapid dose fall-off characteristics. The application of 3D printing facilitates to the development of personalized applicators tailored to the specific contours of the tumor and the surrounding skin. This innovation represents a potential breakthrough in individualized skin surface brachytherapy applicators.[12] The digital design of

Authors' contribution:
A – Research concept and design, B – Collection and/or assembly of data, C – Data analysis and interpretation, D – Writing the article, E – Critical revision of the article, F – Final approval of the article.

essential structures and the rapid manufacturing of required forms using cost-effective technology and materials make this approach not only viable but promising. The imperative of ensuring quality assurance (QA) procedures in radiotherapy cannot be overstated. Regardless of the formalised approach in the treatment planning system (TPS), independent dose verification remains recommended. Dose verification assumes a pivotal role in the treatment process, mitigating errors, enhancing treatment efficiency, and minimizing adverse effects on patients. Various verification methods are employed to achieve this critical objective, encompassing radiochromic film[13-19], ionization chamber[20-24], thermoluminescent dosimeters (TLD)[25-28], gel dosimetry[29-33], independent secondary dose calculation[34-39] and others. The focus is specifically on high-dose rate (HDR) brachytherapy with individual 3D-printed applicators. The primary goal encompasses the evaluation of quantitative dosimetry analysis and a comprehensive assessment of treatment plan parameters.

Materials and methods

The primary objective of this research is to conduct a comparative analysis between dose calculations for brachytherapy calculated as if the sources are in water derived from BrachyVision v16.1 (Varian Medical Systems, Palo Alto, CA) and the independent secondary dose calculation software with brachytherapy module RadCalc (RC) v7.2 (LAP, Germany). The comparison between the TPS and the independent checking software RC was undertaken for various reasons. It serves as a quality assurance measure, ensuring the accuracy and reliability of the TPS in clinical applications. This verification process instills confidence in the precision of dose calculations, supporting the clinical validity of generated treatment plans. The evaluation of system performance identifies areas for potential improvement. Additionally, the comparison aids in optimizing treatment plans for enhanced precision. The comprehensive treatment plan parameter evaluation was presented and analyzed based on clinically applied plans. Various parameters were compared, including the dose disparity between the TPS and independent checking software calculations. The values of parameters V_{100}, V_{150}, V_{200}, and D_{90}, as determined by the TPS and RC, were also scrutinized. The analysis further encompassed parameters such as coverage index (CI), dose non-uniformity ratio (DNR), mean treatment depth, treatment time, and the Gamma parameter, along with the local Gamma for values of 1%/1mm, 2%/2mm, and 3%/3mm. Dose calculations are based on the 192-Ir GammaMed HDR Plus source. In the case of the RC software, the model described in publication[40] has been implemented. Using either Prusa Mini or Prusa iMk3+ 3D printers with fused deposition modeling, all 3D printed applicators were crafted from polylactic acid (PLA) by Fiberology. PLA is renowned as one of the most prevalent and user-friendly printing materials. Its ease of use extends to a relatively swift printing process, contributing to its popularity among users. The versatility and accessibility of PLA make it an excellent choice for a variety of printing applications. The .stl file of the applicator was generated through software that converted the Digital Imaging and Communications in Medicine (DICOM) file of the prepared structure in TPS. The Prusa Slicer software was then employed to convert the .stl file into g-code. For most masks, printing parameters included a speed of 0.15, 100% infill, and a printing speed ranging from 25 to 80 mm/s, depending on the movement type of the heating nozzle. Manual adjustments were made to the supports of all applicators to minimize potential defects on the applicator surface while ensuring that the g-code was fully printable. All statistical analyses, along with the described formulas and charts, have been presented below. At our clinic, RadCalc is an essential software tool utilized in radiation therapy treatment planning, including brachytherapy. It employs algorithms to calculate radiation dose distributions. Task Groups, such as TG-43, provide guidelines and recommendations for brachytherapy dose calculations. RadCalc utilizes input data such as radiation source parameters to perform accurate dose calculations. The software compares calculated dose distributions to expected values from the treatment plan. Discrepancies beyond predefined tolerances trigger further investigation. Its role in verifying treatment plans before patient treatment contributes to improved safety and outcomes. RadCalc, employed in our clinic, plays a crucial role in ensuring the accuracy and reliability of radiation therapy delivery in brachytherapy.

Results and discussion

For 20 patient plans, compliance with the TPS was compared with an independent checking software. The dose difference between the TPS and RC was determined for 3-5 catheters at the surface of the printed applicator and treated tumor. Markings were made at three points in the catheter (low, middle, top). **Figure 1** shows the frequency of the result as a function of the dose difference expressed as a percentage.

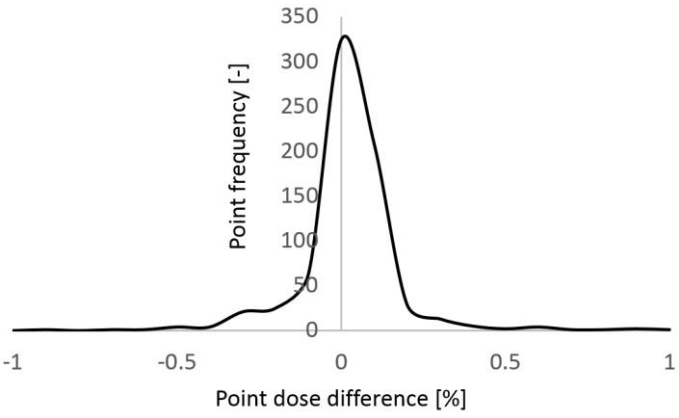

Figure 1. Point dose differences for 20 patient plans.

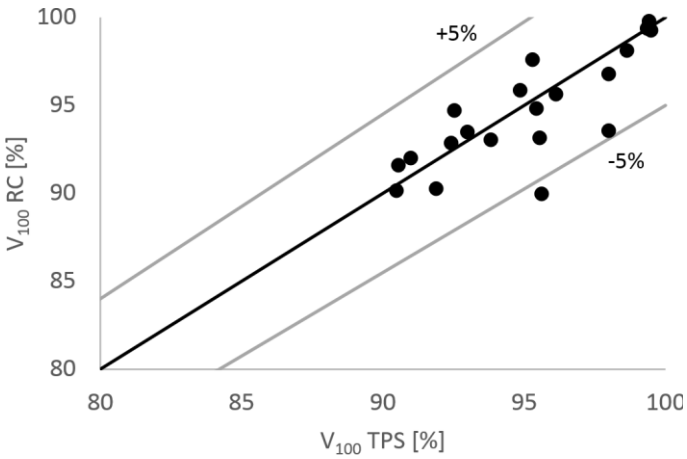

Figure 2. Parity plot for V_{100} obtained for TPS and RC.

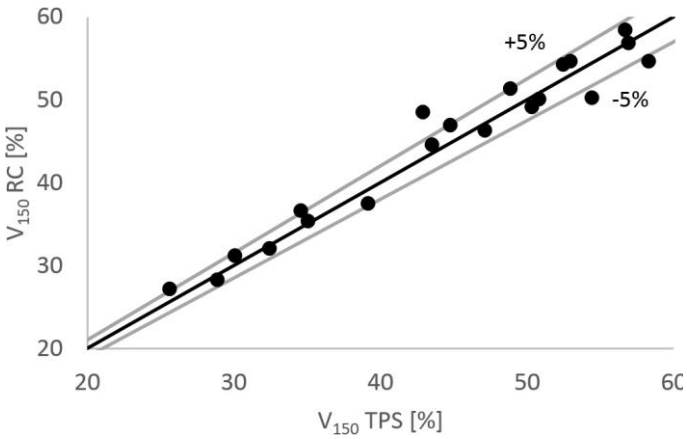

Figure 3. Parity plot for V_{150} obtained for TPS and RC.

Based on the examination of **Figure 1**, it can be deduced that the distribution closely approximates a normal distribution characterized by a mean value of 0.05% and a standard deviation of 0.26%. Such relatively small values of the mean value and standard deviation indicate a very high compliance of the TPS with an RC software, which is very beneficial from a clinical point of view.

Next, the values of parameters V_{100}, V_{150} and V_{200} determined by the TPS and RC were compared. The comparison of these results is presented using a parity plot, where one axis corresponds to the values obtained for the TPS, and the other to the values obtained by an RC. Full compliance with the data on such a chart is achieved when the points are arranged along the straight line $y=x$ (marked with a black line on the charts). Gray lines on these charts mark the area in which the analyzed results do not deviate from $y=x$ by more than 5%. The results for V_{100}, V_{150} and V_{200} are shown in **Figures 2-4** and **Table 1**, respectively.

Analyzing **Figures 2-4** and **Table 1** regarding the parameters V_{100}, V_{150} and V_{200}, it can be concluded that the compliance between the TPS and the results obtained in RC is high. Most results fall within the 5% compliance area. The highest compliance is obtained for the V_{100} parameter, and the lowest for V_{200}. It is worth emphasizing, however, that even for V_{200}, the differences between TPS and RC are relatively small and generally have no clinical significance.

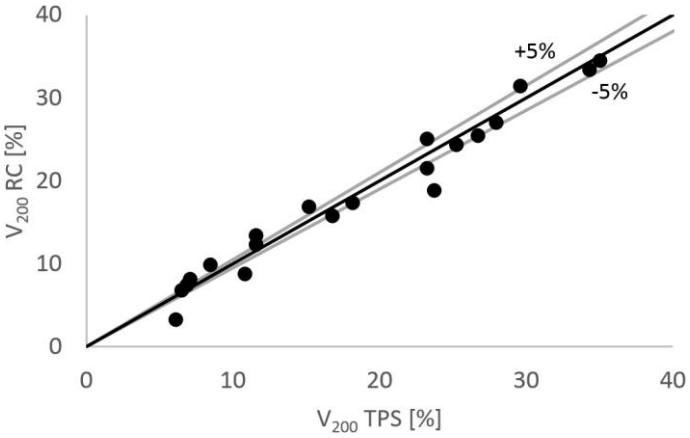

Figure 4. Parity plot for V_{200} obtained for TPS and RC.

Table 1. Comparison between V_{100}, V_{150} and V_{200} obtained for TPS and for RC.

	Mean value [%]	Standard deviation [%]
V_{100} TPS	95.09	2.97
V_{100} RC	94.55	3.06
Difference between TPS and RC for V_{100}	0.01	0.02
V_{150} TPS	44.34	10.01
V_{150} RC	44.61	9.73
Difference between TPS and RC for V_{150}	0.27	2.15
V_{200} TPS	18.48	9.36
V_{200} RC	17.96	9.18
Difference between TPS and RC for V_{200}	0.52	1.72

In a further step, the D_{90} values obtained for the TPS and those calculated by RC were compared. The same method of data presentation and analysis was adopted as for the V_{100}, V_{150} and V_{200} parameters. The comparison results are presented in **Figure 5** and **Table 2**.

Analyzing **Figure 5** and **Table 2** regarding the D_{90} parameter, it can be concluded that the compliance between the TPS and RC is high. The vast majority of results fall within the 5% compliance area. The differences between the values obtained in TPS and RC are relatively small and have no clinical significance.

The next stage of work was the analysis of the CI parameter, which is defined by the formula:

$$CI = \frac{PTV_{dref}}{V_{PTV}} \quad \text{Eq. 1}$$

where, PTV_{dref} – is the reference target volume (taken as volume receiving 100% of the prescribed dose), d_{ref} – volume receiving 100% of the prescribed dose irrespective of the target delineated (derived by generating a structure of volume receiving 100% dose) and V_{PTV} – is the target volume. The expected value of the CI parameter is 1. Therefore, the analysis of the results was performed again using a parity plot in **Figure 6**, plotting the dependence of V_{PTV} and PTV_{dref}. In such a coordinate system, the points should lie on a straight line $V_{PTV} = PTV_{dref}$.

The analysis of **Figure 6** indicates a high compliance of the obtained results with the expected values, i.e. the value of the CI parameter of 1. The data plotted on the parity plot are characterized by a high determination coefficient $R^2 = 0.984$.

In the next step, we assessed the compliance of the DNR parameter which is defined by the formula:

$$DNR = \frac{V_{150}}{V_{100}} \quad \text{Eq. 2}$$

where, V_{150} and V_{100} – are respectively volumes of isodoses equal to 150% and 100%. The described parameter is specified for the TPS and RC software. Again, the data are presented using a parity plot, **Figure 7**, and the numerical data are presented in **Table 3**.

Analyzing **Figure 7** and **Table 3** regarding the DNR parameter, it can be concluded that the agreement between the TPS and the results obtained in the RC is high. The majority of results fall within the 5% compliance area. The differences between the values obtained in TPS and RC are relatively small and have no clinical significance.

Table 3. Comparison between DNR obtained for TPS and for RC.

	Mean value [-]	Standard deviation [-]
DNR TPS	0.47	0.09
DNR RC	0.46	0.10
Difference between TPS and RC	0.01	0.02

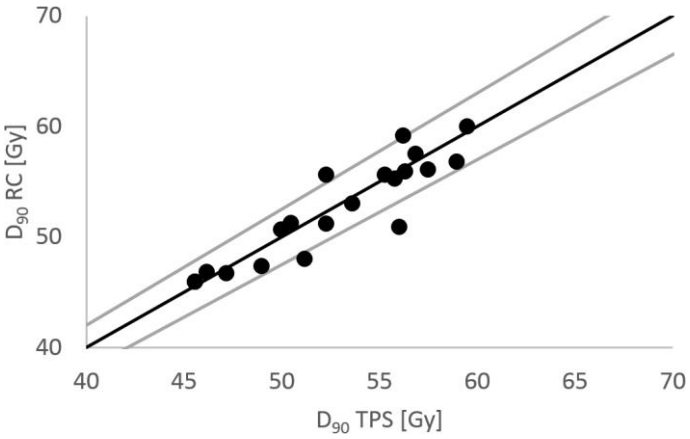

Figure 5. Parity plot for D_{90} obtained for TPS and RC.

Table 2. Comparison between D_{90} obtained for TPS and for RC.

	Mean value [Gy]	Standard deviation [Gy]
D_{90} TPS	52.81	4.37
D_{90} RC	52.45	4.49
Difference between TPS and RC for D_{90}	0.35	1.85

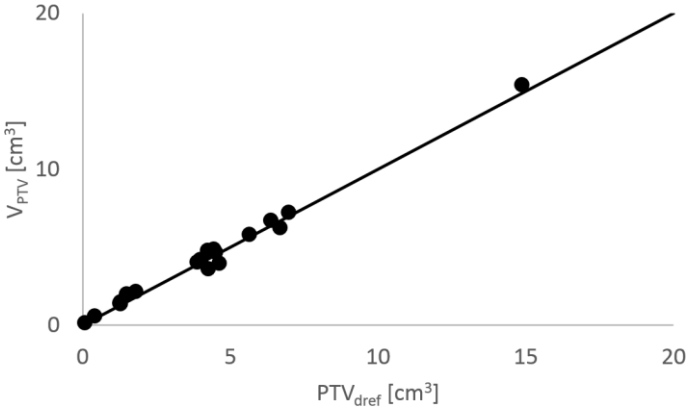

Figure 6. Parity plot for V_{PTV} and PTV_{dref} as an analysis of CI parameter.

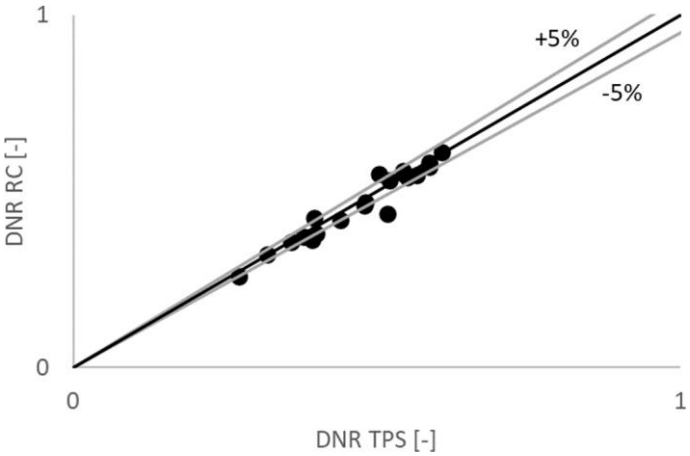

Figure 7. Parity plot for DNR obtained for TPS and RC.

For checking the significance of differences between the values V_{100}, V_{150}, V_{200}, D_{90}, CI, and DNR determined by TPS and by RC, the Student's t-test was applied. In all these cases, there was a dataset with a sample size of 20. The null hypothesis was that the difference between the results for TPS and RC equals zero. The degrees of freedom were 19. A confidence level of α=0.05 was adopted. Under these conditions, in all considered cases, the critical region was within the limits $t_\alpha = (-\infty, -2{,}09) \cup (2.09, +\infty)$. **Table 4**, the test values calculated from the following relationship were compiled:

$$t_e = \frac{\bar{x}-\mu_0}{\sigma}\sqrt{n} \qquad \text{Eq. 3}$$

where $\bar{x}$ is the sample mean, μ_0 is the specified value of the sample, σ is the standard deviation and *n* is the sample size.

The analysis of **Table 4** allows us to conclude that for the analyzed parameters, the differences in values determined for TPS and RC are not statistically significant.

The mean treatment depth was also compared to the corresponding VPTV volume value. The results are summarized in **Figure 8**.

In **Figure 8** it can be seen that as the treatment depth increases, the V_{PTV} volume increases. This is an expected observation. However, what is interesting is that this increase is proportional to the root of depth.

The Gamma parameter was also analyzed, i.e. the passing rate was checked - matching the TPS with the plan calculated by RC. The expected value of the match is 100%. The results of the obtained local Gamma parameter for the values of 1%/1mm, 2%/2mm and 3%/3mm are presented collectively in **Figure 9** and separately in **Table 5**.

The analysis of **Figure 9** and **Table 5** allows us to conclude that the correlation between the TPS and the results of RC is very high. The average Gamma value is 99.91%, with an expected value of 100%, and the average standard deviation is 0.11%. Additionally, we observe that for more restrictive gamma criteria, the results are less favorable, whereas for less restrictive criteria, the outcomes are more favorable, aligning with theoretical expectations.

The last relationship analyzed was the relationship between treatment time and V_{PTV} volume. It can be expected that the larger the volume exposed to a radioactive source, the longer the treatment time. **Figure 10** shows the relationship between treatment time and V_{PTV} volume obtained in treatment plans for 20 patient plans.

Table 4. The significance of differences between TPS and RC determined using the Student's t test.

Parameter	t_α	t_e	Significance
V_{100}	$(-\infty, -2.09) \cup (2.09, +\infty)$	1.29	NO
V_{150}	$(-\infty, -2.09) \cup (2.09, +\infty)$	-0.56	NO
V_{200}	$(-\infty, -2.09) \cup (2.09, +\infty)$	1.35	NO
D_{90}	$(-\infty, -2.09) \cup (2.09, +\infty)$	0.85	NO
CI	$(-\infty, -2.09) \cup (2.09, +\infty)$	-1.37	NO
DNR	$(-\infty, -2.09) \cup (2.09, +\infty)$	1.46	NO

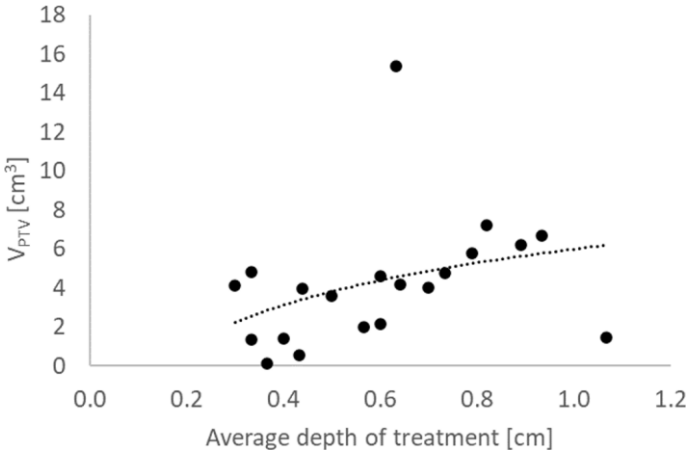

Figure 8. The relationship between average depth of treatment and VPTV.

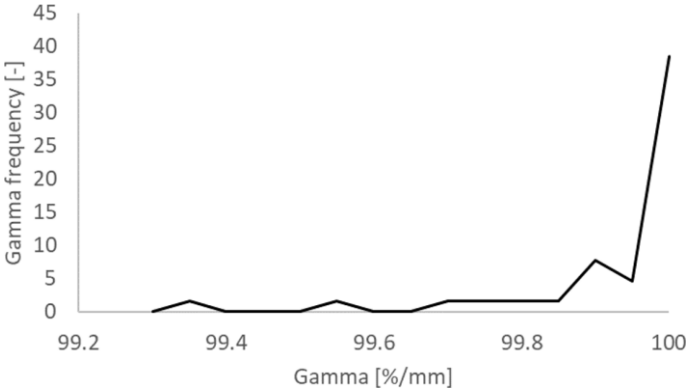

Figure 9. Gamma values for 20 patient plans (for local Gamma 1%/1mm, 2%/2mm and 3%/3mm).

Table 5. Local Gamma values.

	Local Gamma		
	(1%/1mm)	(2%/2mm)	(3%/3mm)
Mean Value	99.83	99.94	99.97
Standard Deviation	0.16	0.11	0.06

The analysis of **Figure 10** confirms the initial thesis that the treatment time increases with the increase in V_{PTV} volume. **Figure 10** shows that this relationship has a power-law nature (root), which means that the treatment time increases more slowly than proportionally depending on the V_{PTV} volume. This relationship also has clinical advantages due to organ at risk (OAR) protection.

The study compared TPS correlation with RC for 20 patient plans, focusing on dose differences. The analysis indicated a distribution close to normal, with mean a of 0.05% and a standard deviation of 0.26%. These values reflect highly beneficial TPS - RC software correlation. Results for V_{100}, V_{150}, and V_{200} indicate a high overall correlation. V_{100} shows a minimal mean difference of 0.01% with a standard deviation of 0.02%, reflecting the highest agreement. V_{150} has a slightly higher mean difference of 0.27% with a standard deviation of 2.15%, maintaining a reasonable correlation. V_{200} exhibits the lowest, correlation with a mean difference of 0.52% and a standard deviation of 1.72%. In summary, TPS reliably aligns with RC results, with the highest correlation for V_{100} and the lowest for V_{200}. The D_{90} values compared between TPS and RC show a high correlation, with a mean difference of 0.35% and a standard deviation of 1.85%. The CI parameter, indicating conformity with expected values (CI = 1), is strongly supported by a high R^2 value of 0.984. DNR values in TPS and RC exhibit close agreement, with mean values of 0.47% (TPS) and 0.46% (RC). The mean difference is minimal at 0.01%, with low variability (TPS standard deviation 0.09%, RC standard deviation 0.10%). The average Gamma value is 99.91%, slightly below the expected 100%, with a low average standard deviation of 0.11%. Notably, stricter gamma criteria yield less favorable results, while less restrictive criteria produce more favorable outcomes, consistent with theoretical expectations. Doses to OAR in both types of plans from the TPS and RC have been carefully assessed. All doses to OARs are within clinically acceptable tolerances.

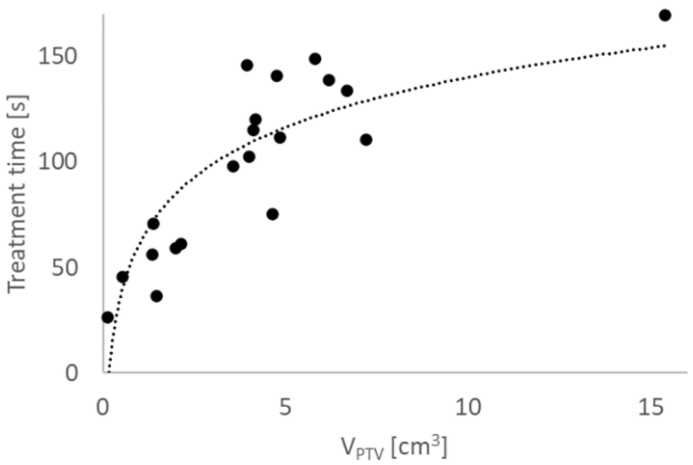

Figure 10. The relationship between time of treatment and V_{PTV}.

Conclusion

Both TPS generated plans and those verified by RC have undergone rigorous evaluation to ensure compliance with established tolerance criteria. The consistent alignment between the TPS and RC results reaffirms the accuracy and reliability of our treatment planning process. The congruence of dosimetric and clinical parameters indicates the suitability of this approach for patient care. These findings instill confidence in the method's efficacy, emphasizing its potential for improved patient outcomes. This validation supports the wider adoption of this treatment strategy, contributing to the overall quality assurance in clinical settings.

References

1. Neville JA, Welch E, Leffell DJ. Management of nonmelanoma skin cancer in 2007. Nat Rev Clin Oncol. 2007;4(8):462-469. https://doi.org/10.1038/ncponc0883
2. Bray F, Ferlay J, Soerjomataram I, Siegel RL, Torre LA, Jemal A. Global cancer statistics 2018: GLOBOCAN estimates of incidence and mortality worldwide for 36 cancers in 185 countries. CA A Cancer J Clinicians. 2018;68(6):394-424. https://doi.org/10.3322/caac.21492
3. Madan V, Lear JT, Szeimies RM. Non-melanoma skin cancer. The Lancet. 2010;375(9715):673-685. https://doi.org/10.1016/s0140-6736(09)61196-x
4. Bath-Hextall F, Leonardi-Bee J, Smith C, Meal A, Hubbard R. Trends in incidence of skin basal cell carcinoma. Additional evidence from a UK primary care database study. Intl Journal of Cancer. 2007;121(9):2105-2108. https://doi.org/10.1002/ijc.22952
5. Gerbaulet A. The GEC ESTRO Handbook of Brachytherapy. ESTRO, Brüssel, 2002
6. Subashi E, Jacobs C, Hood R, Kirsch DG, Craciunescu O. A design process for a 3D printed patient-specific applicator for HDR brachytherapy of the orbit. 3D Print Med. 2020;6(1). https://doi.org/10.1186/s41205-020-00068-3

7. Zhao Y, Moran K, Yewondwossen M, et al. Clinical applications of 3-dimensional printing in radiation therapy. Medical Dosimetry. 2017;42(2):150-155. https://doi.org/10.1016/j.meddos.2017.03.001
8. Park SY, Kang S, Park JM, An HJ, Oh DH, Kim J in. Development and dosimetric assessment of a patient-specific elastic skin applicator for high-dose-rate brachytherapy. Brachytherapy. 2019;18(2):224-232. https://doi.org/10.1016/j.brachy.2018.11.001
9. Diefenhardt M, Chatzikonstantinou G, Meissner M, et al. HDR brachytherapy with individual epithetic molds for facial skin cancer: techniques and first clinical experience. Int J Dermatology. 2021;60(6):717-723. https://doi.org/10.1111/ijd.15492
10. Casey S, Bahl G, Awotwi-Pratt JB. High Dose Rate 192-Ir-Brachytherapy for Basal Cell Carcinoma of the Skin using a 3D Printed Surface Mold. Cureus. Published online June 17, 2019. https://doi.org/10.7759/cureus.4913
11. Arenas M, Sabater S, Sintas A, et al. Individualized 3D scanning and printing for non-melanoma skin cancer brachytherapy: a financial study for its integration into clinical workflow. jcb. 2017;3:270-276. https://doi.org/10.5114/jcb.2017.68134
12. Bielęda G, Chicheł A, Boehlke M, et al. 3D printing of individual skin brachytherapy applicator: design, manufacturing, and early clinical results. jcb. 2022;14(2):205-214. https://doi.org/10.5114/jcb.2022.114353
13. Oare C, Wilke C, Ehler E, Mathew D, Sterling D, Ferreira C. Dose calibration of Gafchromic EBT3 film for Ir-192 brachytherapy source using 3D-printed PLA and ABS plastics. 3D Print Med. 2019;5(1). https://doi.org/10.1186/s41205-019-0040-4
14. Gholami S, Mirzaei HR, et al. A novel phantom design for brachytherapy quality assurance. IJRR. 2016;14(1):67-71. https://doi.org/10.18869/acadpub.ijrr.14.1.67
15. Hsu SM, Wu CH, Lee JH, et al. A Study on the Dose Distributions in Various Materials from an Ir-192 HDR Brachytherapy Source. Deutsch E, ed. PLoS ONE. 2012;7(9):e44528. https://doi.org/10.1371/journal.pone.0044528
16. Sinnatamby M, Nagarajan V, Kanipakam RS, Karunanidhi G, Neelakandan V, Kandasamy S. Verification of Radiation Fluence using Stack Film in HDR Brachytherapy with Heterogeneity Algorithm. JCDR. Published online 2018. https://doi.org/10.7860/jcdr/2018/36733.12258
17. Palmer AL, Bradley D, Nisbet A. Evaluation and implementation of triple-channel radiochromic film dosimetry in brachytherapy. J Applied Clin Med Phys. 2014;15(4):280-296. https://doi.org/10.1120/jacmp.v15i4.4854
18. Devic S. Radiochromic film dosimetry: Past, present, and future. Physica Medica. 2011;27(3):122-134. https://doi.org/10.1016/j.ejmp.2010.10.001
19. Bielęda G, Marach A, Boehlke M, Zwierzchowski G, Malicki J. 3D-printed surface applicators for brachytherapy: a phantom study. jcb. 2021;13(5):549-562. https://doi.org/10.5114/jcb.2021.110304
20. Wolfsberger LD, Wagar M, Nitsch P, Bhagwat MS, Zygmanski P. Angular dose dependency of MatriXX TM and its calibration. J Applied Clin Med Phys. 2010;11(1):241-251. https://doi.org/10.1120/jacmp.v11i1.3057
21. Austerlitz C, Campos CAT. A BrachyPhantom for verification of dose calculation of HDR brachytherapy planning system. Medical Physics. 2013;40(11). https://doi.org/10.1118/1.4826170
22. Yoosuf ABM, Jeevanandam P, Whitten G, Workman G, McGarry CK. Verification of high-dose-rate brachytherapy treatment planning dose distribution using liquid-filled ionization chamber array. JCB. 2018;10(2):142-154. https://doi.org/10.5114/jcb.2018.75599
23. Poppe B, Stelljes TS, Looe HK, Chofor N, Harder D, Willborn K. Performance parameters of a liquid filled ionization chamber array. Med Phys. 2013;40(8):082106. https://doi.org/10.1118/1.4816298
24. Sarfehnia A, Kawrakow I, Seuntjens J. Direct measurement of absorbed dose to water in HDR I192r brachytherapy: Water calorimetry, ionization chamber, Gafchromic film, and TG-43. Med Phys. 2010;37(4):1924-1932. https://doi.org/10.1118/1.3352685
25. Gambarini G, Borroni M, Grisotto S, et al. Solid state TL detectors for in vivo dosimetry in brachytherapy. Applied Radiation and Isotopes. 2012;71:48-51. https://doi.org/10.1016/j.apradiso.2012.06.018
26. Avilés Lucas P, Lourenço V, Vermesse D, Cutarella D, Aubineau-Lanièce I. Absorbed dose to water distribution measured around an HDR192Ir brachytherapy source by thermoluminescent dosimeters. Metrologia. 2012;49(5):S228-S230. https://doi.org/10.1088/0026-1394/49/5/s228
27. Bassi S, Berrigan L, Zuchora A, Fahy L, Moore M. End-to-end dosimetric audit: A novel procedure developed for Irish HDR brachytherapy centres. Physica Medica. 2020;80:221-229. https://doi.org/10.1016/j.ejmp.2020.10.005
28. Lambert J, Nakano T, Law S, Elsey J, McKenzie DR, Suchowerska N. In vivo dosimeters for HDR brachytherapy: A comparison of a diamond detector, MOSFET, TLD, and scintillation detector. Medical Physics. 2007;34(5):1759-1765. https://doi.org/10.1118/1.2727248
29. Watanabe Y, Maeyama T, Mochizuki A, et al. Verification of dose distribution in high-dose-rate brachytherapy using a nanoclay-based radio-fluorogenic gel dosimeter. Phys Med Biol. 2020;65(17):175008. https://doi.org/10.1088/1361-6560/ab98d2
30. Venning A, Healy B, Nitschke K, Baldock C. Investigation of the MAGAS normoxic polymer gel dosimeter with Pyrex glass walls for clinical radiotherapy dosimetry. Nuclear Instruments and Methods in Physics Research Section A: Accelerators, Spectrometers, Detectors and Associated Equipment. 2005;555(1-2):396-402. https://doi.org/10.1016/j.nima.2005.09.002
31. Ibbott GS. Applications of gel dosimetry. J Phys: Conf Ser. 2004;3:58-77. https://doi.org/10.1088/1742-6596/3/1/007

32. Senkesen O, Tezcanli E, Buyuksarac B, Ozbay I. Comparison of 3D dose distributions for HDR 192Ir brachytherapy sources with normoxic polymer gel dosimetry and treatment planning system. Medical Dosimetry. 2014;39(3):266-271. https://doi.org/10.1016/j.meddos.2014.04.003
33. Carrara M, Fallai C, Gambarini G, Negri A. Fricke gel-layer dosimetry in high dose-rate brachytherapy. Applied Radiation and Isotopes. 2010;68(4-5):722-725. https://doi.org/10.1016/j.apradiso.2009.09.036
34. Poder J, Corde S. I-125 ROPES eye plaque dosimetry: Validation of a commercial 3D ophthalmic brachytherapy treatment planning system and independent dose calculation software with GafChromic® EBT3 films. Medical Physics. 2013;40(12). https://doi.org/10.1118/1.4828786
35. Pagulayan C, Heng SM, Corde S. Dosimetric validation of the Theragenics AgX-100® I-125 seed for ROPES eye plaque brachytherapy. Australas Phys Eng Sci Med. 2019;42(2):599-609. https://doi.org/10.1007/s13246-019-00761-6
36. Deufel CL, Furutani KM. Quality assurance for high dose rate brachytherapy treatment planning optimization: using a simple optimization to verify a complex optimization. Phys Med Biol. 2014;59(3):525-540. https://doi.org/10.1088/0031-9155/59/3/525
37. Dempsey C. Methodology for commissioning a brachytherapy treatment planning system in the era of 3D planning. Australas Phys Eng Sci Med. 2010;33(4):341-349. https://doi.org/10.1007/s13246-010-0036-2
38. Damato AL, Devlin PM, Bhagwat MS, et al. Independent brachytherapy plan verification software: Improving efficacy and efficiency. Radiotherapy and Oncology. 2014;113(3):420-424. https://doi.org/10.1016/j.radonc.2014.09.015
39. Shirazi MAM, Faghihi R, Siavashpour Z, Nedaie HA, Mehdizadeh S, Sina S. Independent evaluation of an in-house brachytherapy treatment planning system using simulation, measurement and calculation methods. J Applied Clin Med Phys. 2012;13(2):103-112. https://doi.org/10.1120/jacmp.v13i2.3687
40. Ballester F, Puchades V, Lluch JL, et al. Technical note: Monte-Carlo dosimetry of the HDR 12i and Plus sources. Medical Physics. 2001;28(12):2586-2591. https://doi.org/10.1118/1.1420398